

A 60 GHz lens antenna for high-speed short-range communications

© O.V. Minin^{1,2}, I.V. Minin^{1,2}

¹ Tomsk Polytechnic University, Tomsk, Russia

² Siberian State University of Geosystems and Technologies, Novosibirsk, Russia

E-mail: prof.minin@gmail.com

Received July 25, 2024

Revised September 11, 2024

Accepted September 11, 2024

The paper presents the results of experimental studies of a 60 GHz lens antenna, which were aimed at improving the antenna characteristics based on the photon jet effect. It is shown that placing a dielectric cube at the waveguide open end according to the „plug-and-play“ principle leads to an increase in the antenna gain up to 5 dBi without changing the design of the lens antenna itself. When the antenna operates in the „receive“ mode, the gain increase is approximately 7 dB at the frequency of about 67 GHz.

Keywords: photon jet, lens antenna, gain.

DOI: 10.61011/TPL.2025.01.60148.20071

Antennas are among the fundamental components of the millimeter-wave (MMW) and terahertz (THz) imaging, detection and high-speed communication systems. The 60 GHz frequency band is provided free of charge and is used in industrial, scientific and medical applications. However, resonant absorption by oxygen molecules in air causes an increase in the attenuation losses at 60 GHz to above 13 dB/km [1–3]. This attenuation can restrict the range of wireless communications; however, such high losses may be compensated for by using high-gain antennas.

MMW 5G „point–point“ antennas are to be of low profile, low cost and high gain since they may be mainly deployed for small cells in urban environment. Range V (57–66 GHz) is one of the candidates for the 5G small cell communications. For instance, MMW systems at the unlicensed 60 GHz frequency have already been standardized for short-range high-speed communication channels for wireless personal area networks (WPAN) (802.15.3c), wireless streaming of high-definition video (WirelessHD), WiGig networks and „point–point“ communication systems [4,5], as well as for antenna systems for ground terminals of advanced satellite communication systems.

Lens antennas are more attractive for various MMW applications due to the good compromise between the directivity and insertion loss level. To improve the antenna gain and directivity, lenses of various types are used to focus electromagnetic waves [6–9]. In [10], the MMW and THz lens antennas fabricated by 3D printing were investigated; as the antireflective layer, variable-height square dielectric pillars were used. Under this concept it is possible to improve the lens's directivity by introducing a periodic antireflective structure at the air–lens interface. Such lens antennas possess high gains and wide bandwidths with low profiles.

Lens antennas are known to consist of two main components: the lens itself, which focuses the incident energy at the specified point, and radiation receiver; the receiving

part design may be absolutely different, changing from the horn antenna to microstrip antenna and open-ended waveguide [11]. However, the existence of fundamental diffraction limitations prevents the lens antenna from focusing the incident radiation into a spot smaller in size than the diffraction limit; the transverse size of this focusing spot is typically larger than the size of the waveguide open end. This means that a portion of energy focused by the lens gets lost.

The above-mentioned limitations prompted us to propose an alternative approach to constructing an MMW/THz antenna; this approach is characterized by a high degree of integration into already existing antennas according to the „plug-and-play“ principle.

One of the methods for reducing the focal spot size down to the MMW/THz subwavelength range is to use the so-called effect of photonic jet [12,13] generated by an arbitrary-shaped 3D mesoscale dielectric particle [13]. Note that the first experimental confirmation of the photonic jet effect was obtained in the microwave range (see [13] and references therein). Remind that the photonic jet formation (field localization and amplification in the dielectric particle shadow part) is observed under the condition that the particle characteristic size is no less than the incident radiation wavelength [12,13]. The photonic jet effect in the near-field mode for the subwavelength THz imaging was for the first time investigated in [14]. In [15], far-field investigation of the cubic mesoscale structure at both 300 GHz and 24 GHz showed that the far-field gain of such an antenna (14.22 dBi) is 1.9 dB higher than that of a horn antenna of the same size. The radiation pattern widths (FWHMs) were approximately 21 and 34% lower than those for the horn antenna in the E and H planes, respectively. We have also demonstrated wireless data transmission at the 17.5 Gbit/s speed in the 300 GHz band by using a $1.2 \times 1.2 \times 1.36$ mm dielectric cubic antenna. At this frequency, the maximum antenna gain was approximately 15 dBi [16].

At the same time, to our knowledge, so far there has been proposed no solution or study demonstrating utilization of the photonic jet effect in a millimeter-wave dielectric lens antenna, which would allow increasing the antenna gain without modifying the lens itself.

The goal of this study was to demonstrate a method for increasing the lens antenna gain by localizing the field at the input of the receiving waveguide open end with the aid of a mesoscale dielectric particle forming a photonic jet. Using as an example a 3D-printed 60 GHz lens antenna with the feeder in the form of an open-ended circular waveguide [10], we have demonstrated here that placing a cubic mesoscale dielectric particle at the waveguide open-end output increases the gain by approximately 6 dBi.

The experimental 60 GHz MMW lens antenna was based on a diffraction lens described in detail in [10], in which open-ended waveguide WR-15 was used as a lens feed. At the frequency of about 60 GHz, the used dielectric had relative permittivity of $\epsilon_r = 2.9$ and loss tangent of $\tan \delta = 0.01$. As the lens unit cells for phase compensation, variable-height square dielectric columns were used. To minimize reflection from the lens, an antireflection layer was created in the form of an artificial dielectric consisting of rectangular columns whose geometric dimensions were selected as per recommendations of [17]. The column dielectric permittivity and thickness were $\epsilon_{AR} \approx 1.7$ and $t \approx 0.95$ mm, respectively. The lens developed had a square aperture with 19×19 rectangular dielectric columns providing the necessary phase compensation (Fig. 1). The focal length to lens diameter ratio (F/D) was 0.42. The lens was fabricated by using a 3D printer with the base resolution of $42 \times 42 \times 28 \mu\text{m}$ along the x , y and z axes, respectively. To minimize the sidelobe level, optimization of the diffractive lens Soret–Minin–Webb reference phase was used [8,9,18]. A more detailed description of the lens is given in [10].

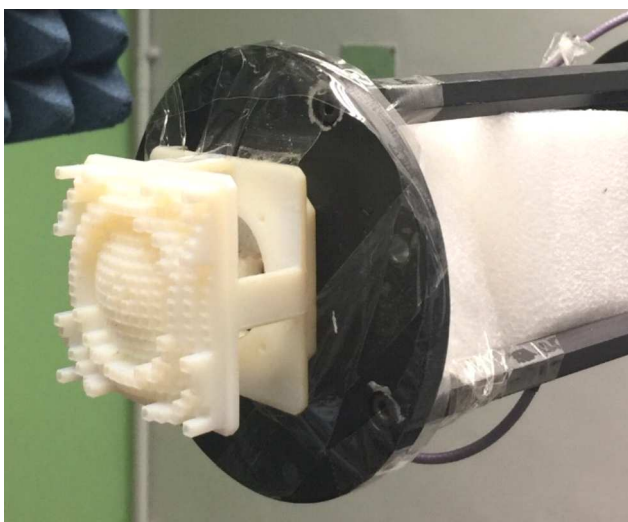


Figure 1. A 60 GHz antenna fabricated by 3D printing.

The radiation pattern and gain of the proposed antenna were measured using planar-scanning near-field system NSI2000 [19] in an anechoic chamber. The measured gain of the original antenna shown in Fig. 1 ranges from 19.4 to 23.5 dBi; therewith, the sidelobe levels are below -18 and -14 dB in the H and E planes, respectively. When the mesoscale dielectric particle (fluoroplastic, cube edge of 5 mm) is installed at the circular waveguide open end (Fig. 2), the antenna gain increases significantly (Fig. 3, *a*). Thus, the measured gain of the antenna with the cubic particle at the waveguide open end ranges from 19.4 to 23.5 dBi, the sidelobe levels being below -18 and -14 dB in the H and E planes, respectively.

The figure clearly shows that the effect of the gain increase is observed at a frequency exceeding 60 GHz. The source of such a behavior of the gain is the size of the dielectric cubic particle: at this frequency the cube edge is equal to one wavelength, while at higher frequencies the cube effective dimensions are greater than the wavelength (Fig. 3). In this case, the benefit from the gain of antenna with a simple dielectric particle at the waveguide open end is up to 4 dB. As the measurements have shown, placing a dielectric cube on the waveguide open end leads to narrowing of the radiation pattern of the antenna's main scattering lobe by approximately 1.4 times.

Finally, Fig. 3, *b* presents a frequency characteristic of increasing antenna sensitivity in case a cubic particle is used as an additional receiving element to be installed at the waveguide open end. The frequency characteristic is normalized to that of the open waveguide. As the feed antenna, a conical horn connected to a waveguide was used. The measured feed wavefront parameters have shown that the wave incident on the lens may be considered as plane. Higher sensitivities were achieved in the higher-frequency part of the range under consideration, while the gain increase by approximately 7.3 dB was observed at the frequency of about 67 GHz. These characteristics are approximately the same as in the case of placing mesoscale particles of various shapes (sphere, cube) directly on the THz receiver [20]. It is worth noting that, when a cube is used, the signal gain does not exhibit resonant characteristics, which indicates its broadband nature. The latter is very important for wireless MMW and THz communication applications.

The concept of modifying the lens antenna design, which was briefly discussed above, is applicable to other types of antennas; this gives a „new life“ and opens up new possibilities for the existing and future MMW and THz antennas. The main factor restricting the increase in the mesoscale particle operating frequency for various-type antennas is the loss in the dielectric material. Nevertheless, such a solution has certain advantages at least up to frequencies of about 300 GHz; among those advantages there are a wide bandwidth, high directivity, and small pattern FWHM with small physical footprint. The demonstrated here „plug-and-play“ approach to the lens antenna modification may be an

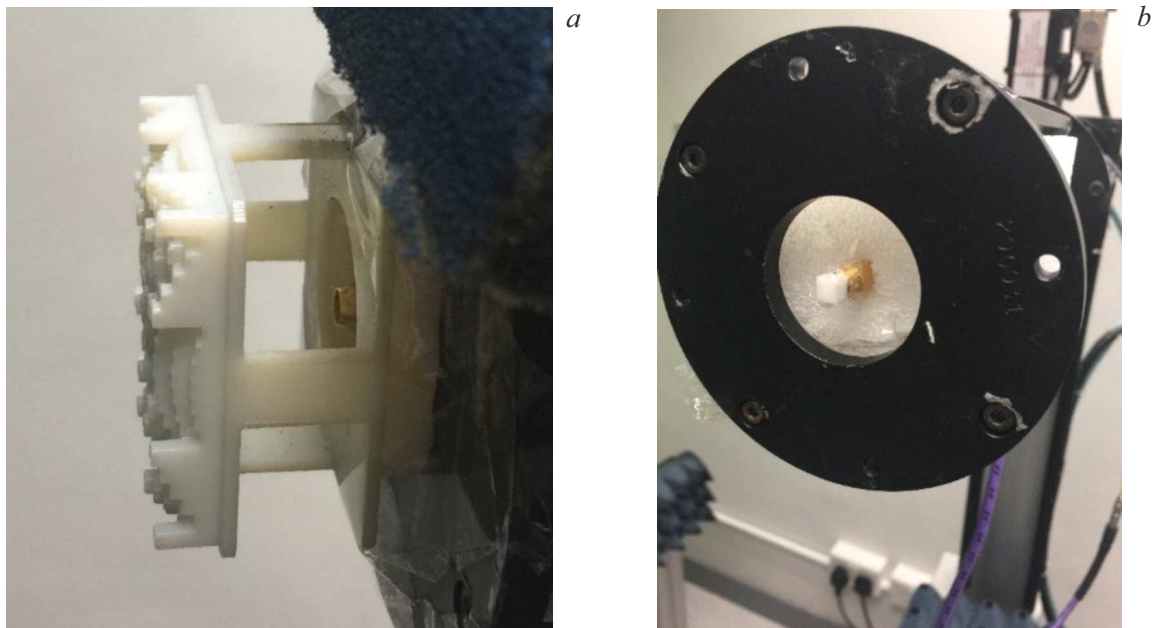


Figure 2. *a* — original antenna with an open-ended circular waveguide; *b* — circular waveguide with a mesoscale cubic particle.

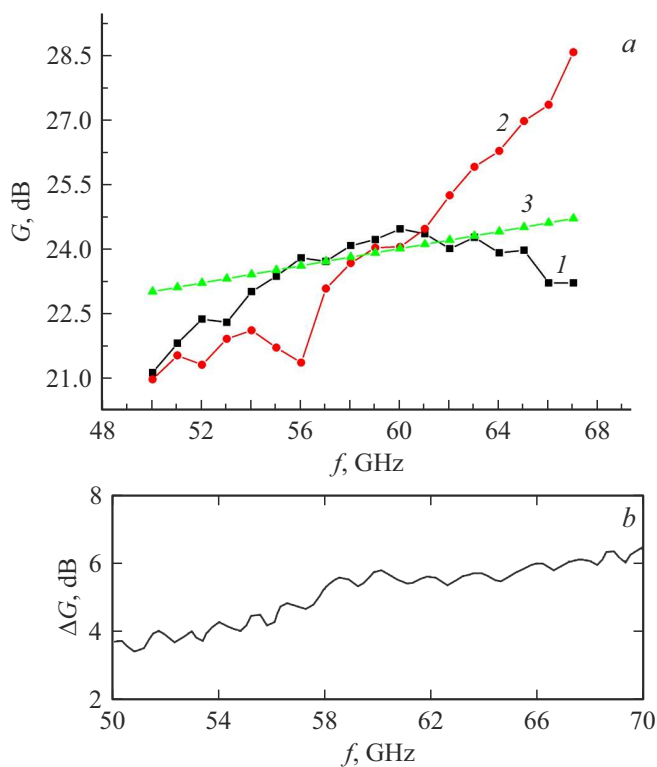


Figure 3. *a* — modified gain of antennas with circular open-ended waveguide (1) and waveguide with a cubic particle (2). 3 — gain of a conventional horn antenna. *b* — increase in sensitivity of the receiving antenna with the cube at the receiving waveguide open end.

important step towards practical application of MMW/THz communication, radar and imaging systems.

Acknowledgements

The authors express their gratitude to Prof. Chi Hou Chan for inviting in 2016 to visit his laboratory and providing the opportunity to conduct relevant experiments.

Funding

The study was partially supported by the Tomsk Polytechnic University Development Program.

Conflict of interests

The authors declare that they have no conflict of interests.

References

- [1] D.S. Makarov, M.Yu. Tretyakov, P.W. Rosenkranz, J. Quant. Spectr. Rad. Transfer, **243**, 106798 (2020). DOI: 10.1016/j.jqsrt.2019.106798
- [2] M. Arvas, M. Alsunaidi, in *2019 IEEE Int. Symp. on antennas and propagation and USNC-URSI radio science meeting* (IEEE, 2019), p. 2127–2128. DOI: 10.1109/APUSNCURSINRSM.2019.8888884
- [3] *Ultra-wideband and 60 GHz communications for biomedical applications*, ed. by M.R. Yuce (Springer, N.Y., 2014). DOI: 10.1007/978-1-4614-8896-5
- [4] A. Jabbar, M.A. Jamshed, Q. Abbasi, M.A. Imran, M. Ur-Rehman, in *2023 IEEE Int. Symp. on antennas and propagation and USNC-URSI radio science meeting (USNC-URSI)* (IEEE, 2023), p. 1567–1568. DOI: 10.1109/USNC-URSI52151.2023.10237884

- [5] X. Tie, K. Ramachandran, R. Mahindra, in *Passive and active measurement (PAM 2012)*, ed. by N. Taft, F. Ricciati. Ser. Lecture Notes in Computer Science (Springer, Berlin–Heidelberg, 2020), vol. 7192, p. 147–157. DOI: 10.1007/978-3-642-28537-0_15
- [6] D. Zelenchuk, V. Kirillov, C. Kärnfelt, F. Gallée, I. Munina, *Electronics*, **12** (11), 2354 (2023). DOI: 10.3390/electronics12112354
- [7] N. Muckermann, J. Barowski, N. Pohl, *Int. J. Microw. Wirel. Technol.*, published online (2023). DOI: 10.1017/S1759078723001472
- [8] I.V. Minin, O.V. Minin, *Diffractional optics of millimetre waves* (CRC Press, Boca Raton, 2004). DOI: 10.1201/9781420034486
- [9] I.V. Minin, O.V. Minin, *Basic principles of Fresnel antenna arrays* (Springer, Berlin–Heidelberg, 2008). DOI: 10.1007/978-3-540-79559-9
- [10] H. Yi, S.-W. Qu, K.-B. Ng, C.H. Chan, X. Bai, *IEEE Trans. Antennas Propag.*, **64** (2), 442 (2016). DOI: 10.1109/TAP.2015.2505703
- [11] S.S. Dhillon, M.S. Vitiello, E.H. Linfield, A.G. Davies, M.C. Hoffmann, J. Booske, C. Paoloni, M. Gensch, P. Weightman, G.P. Williams, E. Castro-Camus, D.R.S. Cumming, F. Simoens, I. Escorcia-Carranza, J. Grant, S. Lucyszyn, M. Kuwata-Gonokami, K. Konishi, M. Koch, C.A. Schmuttenmaer, T.L. Cocker, R. Huber, A.G. Markelz, Z.D. Taylor, V.P. Wallace, J.A. Zeitler, J. Sibik, T.M. Korter, B. Ellison, S. Rea, P. Goldsmith, K.B. Cooper, R. Appleby, D. Pardo, P.G. Huggard, V. Krozer, H. Shams, M. Fice, C. Renaud, A. Seeds, A. Stöhr, M. Naftaly, N. Ridler, R. Clarke, J.E. Cunningham, M.B. Johnston, *J. Phys. D: Appl. Phys.*, **50** (4), 043001 (2017). DOI: 10.1088/1361-6463/50/4/043001
- [12] O.V. Minin, I.V. Minin, *Opt. Quantum Electron.*, **49** (10), 326 (2017). DOI: 10.1007/s11082-017-1165-6
- [13] I.V. Minin, O.V. Minin, *Diffractional optics and nanophotonics. Resolution below the diffraction limit* (Springer, Cham, 2016). DOI: 10.1007/978-3-319-24253-8
- [14] H.H. Nguyen Pham, S. Hisatake, O.V. Minin, T. Nagatsuma, I.V. Minin, *APL Photon.*, **2** (5), 056106 (2017). DOI: 10.1063/1.4983114
- [15] Y. Samura, K. Horio, V. Antipov, S. Shipilov, A. Eremeev, O.V. Minin, I.V. Minin, *IEEE Antennas Wirel. Propag. Lett.*, **18** (9), 1828 (2019). DOI: 10.1109/LAWP.2019.2930820
- [16] K. Yamada, Y. Samura, O.V. Minin, A. Kanno, N. Sekine, J. Nakajima, I.V. Minin, S. Hisatake, *Front. Commun. Net.*, **2**, 702968 (2021). DOI: 10.3389/frcmn.2021.702968
- [17] A.V. Stankovsky, E.A. Strigova, S.V. Polenga, Yu.P. Salomatov, *Tech. Phys. Lett.*, **50** (7), 63 (2024). DOI: 10.61011/TPL.2024.07.58731.19888.
- [18] I.V. Minin, O.V. Minin, *Sov. Letters to the J. Tech. Phys.*, **15** (23), 29–33 (1989).
- [19] *Near-field Systems, Inc., NSI2000* [Electronic source]. <http://www.nearfield.com/products/Software.aspx>
- [20] O.V. Minin, I.V. Minin, Y. Li, J. Han, *PIER Lett.*, **101**, 29 (2021). DOI: 10.2528/PIERL21071901

Translated by EgoTranslating